Resonances and Synchronization in Two Coupled Oscillators with Stick-Slip Vibrations and Spring Pendulums

Dariusz Grzelczyk[1*], Jan Awrejcewicz[1]

Abstract

We study the dynamical behavior of a system of two coupled mechanical oscillators with spring pendulums and driven by a stick-slip induced vibrations. Each of the oscillator consists of the body placed onto a moving belt/foundation, mechanical coupling associated with the body load pressed the belt depending on the body movement as well as suspended spring pendulum. In addition, the influence of the presence of additional electric/electromagnetic forces acting on the pendulums are analyzed. Different kinds of resonance behavior can be found in the studied system, even if it is simplified to a single degree-of-freedom system. As a result, due to many degrees-of-freedom and strong nonlinearity and discontinuity of the considered system, novel nonlinear dynamical phenomena occur, both near and beyond to the resonance. The motion analysis for different cases is carried out by employing standard numerical methods dedicated for nonlinear systems, including both qualitative and quantitative methods, as well as original animations of the system dynamics created in Mathematica. Understanding the role of coupling, transition between fixed points and energy transition in the considered system can be potentially applied in other similar systems, especially in real electro-mechanical systems, power system or in structural engineering.

Keywords
Spring pendulum, swimming pendulum, stick-slip vibrations

[1] Lodz University of Technology, Department of Automation, Biomechanics and Mechatronics,
1/15 Stefanowski Street, Lodz, Poland
* Corresponding author: dariusz.grzelczyk@p.lodz.pl

Introduction

The behavior of the nonlinear and discontinuous dynamical systems is of great interest of many researchers. The steady-state motion of those systems is usually observed and this regime of motion is commonly investigated. In dynamical systems with stable and unstable fixed points it may happen that the unsteady or transient behavior also should be taken into account. In numerous cases, in the non-steady vibrations intensive energy exchange between the coupled elements of the system and either external source, or environment is observed. Especially, in systems with many degrees of freedom also energy exchange between parts of the structure or between modes may often occur. The mentioned phenomena are widely reported and discussed in scientific literature, for instance in references [1, 2, 3].

Motivated by cited references and many others, in this paper the dynamics of two coupled oscillators with stick-slip vibrations and spring pendulums is investigated. The proposed mechanical system serves as a very good example of a study of non-linear phenomena exhibited by two coupled mechanical oscillators. Main goal of the paper is to calculate all stable and unstable fixed points of the system and to investigate its dynamics. In our future work the behavior of the analysed system will be monitored via standard time histories, phase portraits, bifurcation diagram, Lyapunov exponents as well as power spectra densities in order to detect some interesting results (periodic, quasi-periodic, chaotic and hyper-chaotic orbits, the occurrence of multiple resonances, anti-resonance, synchronization effect, energy transition between oscillators, or different scenarios of transition from regular to chaotic motion, etc).

1. Model of the Considered System

Figure 1 shows the model of the considered planar system of two ($i = 1,2$) coupled mechanical oscillators embedded in the Earth gravitational field ($g = 9.81 \mathrm{m/s}^2$). The distance between the mentioned oscillators are equal to L. The bodies with masses M_i and displacements x_i and $y_i = 0$ are laying on a belt (serving as a foundation) which is moving with a constant velocity v_{dr}. Between these masses dry frictions F_{fri} occur which are governed by nonlinear functions of the relative velocities $v_{dr} - \dot{x}_i$ of the belt and the bodies, respectively. The mentioned masses are coupled with each other by a spring-damper element with coefficients k and c, respectively. Moreover, they are also coupled by other spring-damper elements (with coefficients $k_{ix}, c_{ix}, k_{iy}, c_{iy}$) with rigid bodies with moments of inertia B_i and described by rotational angles θ_i. These bodies can rotate about the pivot points, where torsional spring-damper elements k_i, c_i are applied. Bodies with moments of inertia B_i are also characterized by the lengths l_{ix}, l_{iy} and they are pressed masses M_i to the belt. Masses M_i are coupled with spring-damper pendulums which motion are governed by the angles φ_i and displacements Δx_i. The above mentioned pendulums have point masses m_i, initial lengths l_{i0}, stiffness coefficients k_{pi} and damping coefficients c_{pi}. In addition, each mass m_i is driven additional by forces $\mathbf{F}_i$ acting as a result of an electrostatic/electromagnetic interaction between the mentioned mass and a body placed under the belt at a distance L_i.
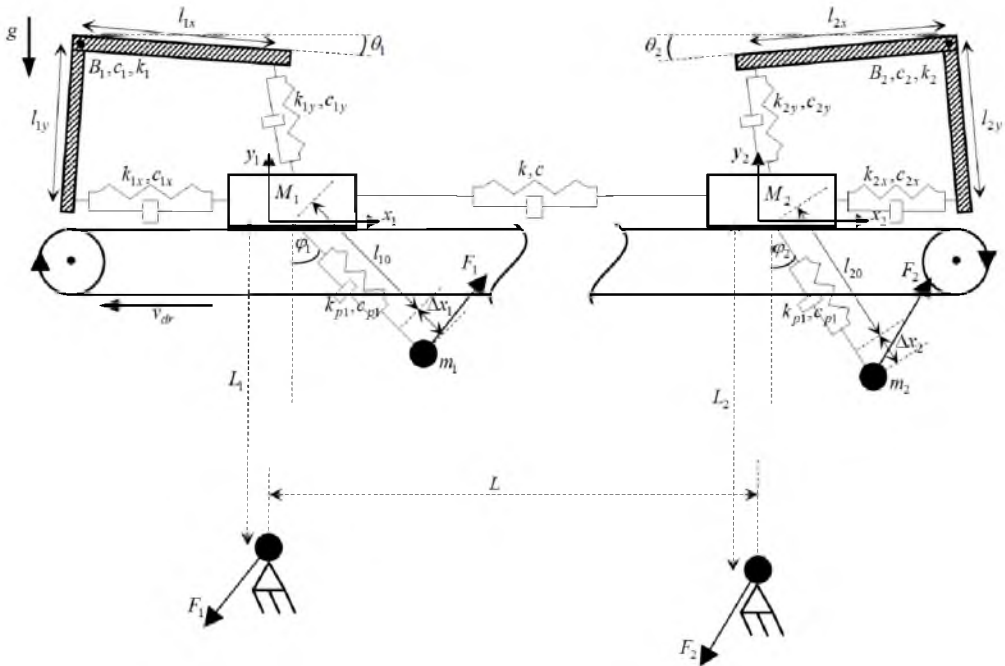

Figure 1. Model of two coupled mechanical oscillators embedded into gravity and electrostatic/electromagnetic field

Equations of motion of the considered system have the following form

$$M_1\ddot{x}_1 = P - P_{1x} + Q_{1x} + F_{fr1}$$
$$M_1\ddot{y}_1 = N_1 - M_1g - P_{1y} - Q_{1y}$$
$$m_1\ddot{x}_{p1} = -Q_{1x} + F_{1x}$$
$$m_1\ddot{y}_{p1} = Q_{1y} - m_1g + F_{1y}$$
$$B_1\ddot{\theta}_1 + c_1\dot{\theta}_1 + k_1\theta_1 = -l_{1y}P_{1x} - l_{1x}P_{1y}$$
$$M_2\ddot{x}_2 = -P + P_{2x} + Q_{2x} + F_{fr2}$$
$$M_2\ddot{y}_2 = N_2 - M_2g - P_{2y} - Q_{2y}$$
$$m_2\ddot{x}_{p2} = -Q_{2x} + F_{2x}$$
$$m_2\ddot{y}_{p2} = Q_{2y} - m_2g + F_{2y}$$
$$B_2\ddot{\theta}_2 + c_2\dot{\theta}_2 + k_2\theta_2 = -l_{2y}P_{2x} - l_{2x}P_{2y}$$

$$(1)$$

where: $P = k(x_2 - x_1) + c(\dot{x}_2 - \dot{x}_1)$, $P_{1x} = k_{1x}(l_{1y}\theta_1 + x_1) + c_{1x}(l_{1y}\dot{\theta}_1 + \dot{x}_1)$, $P_{1y} = k_{1y}l_{1x}\theta_1 + c_{1y}l_{1x}\dot{\theta}_1$, $P_{2x} = k_{2x}(l_{2y}\theta_2 - x_2) + c_{2x}(l_{2y}\dot{\theta}_2 - \dot{x}_2)$, $P_{2y} = k_{2y}l_{2x}\theta_2 + c_{2y}l_{2x}\dot{\theta}_2$, $Q_{1x} = (k_{p1}\Delta x_1 + c_{p1}\Delta\dot{x}_1)\sin\varphi_1$, $Q_{1y} = (k_{p1}\Delta x_1 + c_{p1}\Delta\dot{x}_1)\cos\varphi_1$, $Q_{2x} = (k_{p2}\Delta x_2 + c_{p2}\Delta\dot{x}_2)\sin\varphi_2$, $Q_{2y} = (k_{p2}\Delta x_2 + c_{p2}\Delta\dot{x}_2)\cos\varphi_2$, $x_{p1} = x_1 + (l_{10} + \Delta x_1)\sin\varphi_1$, $y_{p1} = -(l_{10} + \Delta x_1)\cos\varphi_1$, $x_{p2} = x_2 + (l_{20} + \Delta x_2)\sin\varphi_2$, $y_{p2} = -(l_{20} + \Delta x_2)\cos\varphi_2$. Moreover, F_{ix}, F_{iy} are components of forces $\mathbf{F}_i$, while F_{fri} are friction forces between masses M_i and the moving belt.

The friction forces F_{fri} are equal to a scalar product of the nonlinear kinetic friction coefficients $\mu_{ki}(v_{dr} - \dot{x}_i) = \mu_{ist}/(1 + \delta_i | v_{dr} - \dot{x}_i |)$ with parameters δ_i and the reaction normal forces N_i. In our simulations the classical signum function is approximated by the continuous and smooth hiperbolic tangent function with numerical control parameter ε. The friction forces F_{fri} strongly depend on the normal forces $N_i = M_ig + P_{iy} + Q_{iy}$ pressing the masses M_i to the belt. Observe that a numerical simulation result yield the normal force $N_i > 0$, $N_i = 0$ or $N_i < 0$. If $N_i > 0$, then the friction contact between the mass M_i and the belt moving with velocity v_{dr} occurs. In turn, $N_i \leq 0$ means a loss of friction contact between the mass M_i and the belt. This is why in our mathematical model we added a discontinuous "UnitStep" function $\mathbf{1}(N_i)$ describing this phenomenon, being defined as

$$\mathbf{1}(N_i) = \begin{cases} 1 & \text{if} \quad N_i > 0 \\ 0 & \text{if} \quad N_i \leq 0 \end{cases}$$

$$(2)$$

Finally, friction forces F_{fri} are computed employing the following relations

$$F_{fri} = (M_ig + P_{iy} + Q_{iy}) \cdot \tanh\left(\frac{v_{dr} - \dot{x}_i}{\varepsilon}\right) \cdot \frac{\mu_{ist}}{1 + \delta_i | v_{dr} - \dot{x}_i |} \cdot \mathbf{1}(M_ig + P_{iy} + Q_{iy}) \quad (3)$$

In our numerical investigations we also take into account additional interactions acting on the point masses m_j in the following form

$$\mathbf{F}_i = \frac{\kappa_i}{r_i^2} \frac{\mathbf{r}_i}{|\mathbf{r}_i|} \tag{4}$$

with proportionality coefficients κ_i and distances r_i between the bodies. The proposed force $\mathbf{F}_i$ can have both electrostatic or (electro)magnetic nature. After the appropriate transformations, the forces $\mathbf{F}_i$ can be estimated in the following way

$$\mathbf{F}_i = [F_{ix}, F_{iy}]^T = \left[\frac{\kappa_i r_{ix}}{(r_{ix}^2 + r_{iy}^2)^{1.5}}, \frac{\kappa_i r_{iy}}{(r_{ix}^2 + r_{iy}^2)^{1.5}} \right]^T \tag{5}$$

where $r_{ix} = x_{pi}$ and $r_{iy} = y_{pi} + L_i$.

2. Computational Methods

Dimensional equations of motion of the considered system have been solved numerically by the Runge-Kutta method implemented in Mathematica software. In addition, in order to illustrate and understand the obtained results the appropriate animation of the system has been created in Mathematica software (see Fig. 2). In numerical simulations, the following parameters are fixed: $M_1 = M_2 = 1\,\text{kg}$, $v_{dr} = 0.5\,\text{m/s}$, $k = 100\,\text{N/m}$, $c = 10\,\text{N}\cdot\text{s/m}$, $k_{1x} = k_{2x} = 100\,\text{N/m}$, $c_{1x} = c_{2x} = 10\,\text{N}\cdot\text{s/m}$, $k_{1y} = k_{2y} = 100\,\text{N/m}$, $c_{1y} = c_{2y} = 10\,\text{N}\cdot\text{s/m}$, $B_1 = B_2 = 0.1\,\text{kg}\cdot\text{m}^2$, $k_1 = k_2 = 10\,\text{N}\cdot\text{m/rad}$, $c_1 = c_2 = 1\,\text{N}\cdot\text{m}\cdot\text{s/rad}$, $l_{1x} = l_{2x} = 0.5\,\text{m}$, $l_{1y} = l_{2y} = 0.5\,\text{m}$, $m_1 = m_2 = 0.4\,\text{kg}$, $l_{10} = l_{20} = 0.5\,\text{m}$, $k_{p1} = k_{p2} = 100\,\text{N/m}$, $c_{p1} = c_{p2} = 10\,\text{N}\cdot\text{s/m}$, $L_1 = L_2 = 0.8\,\text{m}$, $L = 2\,\text{m}$, $\kappa_1 = \kappa_2 = 1\,\text{N}\cdot\text{m}^2$, $\mu_{1st} = \mu_{2st} = 0.4$, $\delta_1 = \delta_2 = 3\,\text{s/m}$, $\varepsilon = 10^{-4}$ and zero initial conditions are employed. The further reported numerical results are obtained for a set of different parameters. The obtained numerical solutions of the equations of motion presented in the dimensional form are directly applied for animation. However, in our further global numerical analysis (the occurrence of multiple resonances, anti-resonances, synchronization effect, energy transition between oscillators, scenarios of transition from regular to chaotic motion, bifurcation diagrams, Lyapunov exponents, etc.) the non-dimensional equations are taken. Moreover, our future investigations (not reported here) are aimed on getting an approximate asymptotic solution of the non-steady state motion of the considered system using the multiple time scale method [1,3].
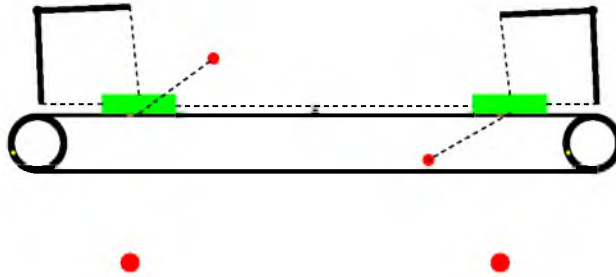

Figure 2. Frame of animation of the considered system presented with the help of Mathematica software (the dashed curves represent spring-damper elements)

3. Numerical Results

First, all stable and unstable fixed points of the considered system are calculated. In the case of $\mu_{1st} = \mu_{2st} = 0$ and $\kappa_1 = \kappa_2 = 0$ the analysed system possesses the following four fixed points:

$$(1): x_1 = 0, x_2 = 0, \Delta x_1 = -m_1 g / k_{p1}, \Delta x_2 = -m_2 g / k_{p2}, \theta_1 = 0, \theta_2 = 0, \varphi_1 = \pi, \varphi_2 = \pi,$$
$$(2): x_1 = 0, x_2 = 0, \Delta x_1 = -m_1 g / k_{p1}, \Delta x_2 = m_2 g / k_{p2}, \theta_1 = 0, \theta_2 = 0, \varphi_1 = \pi, \varphi_2 = 0,$$
$$(3): x_1 = 0, x_2 = 0, \Delta x_1 = m_1 g / k_{p1}, \Delta x_2 = -m_2 g / k_{p2}, \theta_1 = 0, \theta_2 = 0, \varphi_1 = 0, \varphi_2 = \pi, \quad (6)$$
$$(4): x_1 = 0, x_2 = 0, \Delta x_1 = m_1 g / k_{p1}, \Delta x_2 = m_2 g / k_{p2}, \theta_1 = 0, \theta_2 = 0, \varphi_1 = 0, \varphi_2 = 0,$$

and the appropriate system configurations are shown in Fig. 3. In turn, for values of system parameters introduced in Section 2 but without friction forces ($\mu_{1st} = \mu_{2st} = 0$), the system has eight fixed points (obtained numerically). Configurations of the system for the mentioned eight fixed points are presented in Fig. 4.
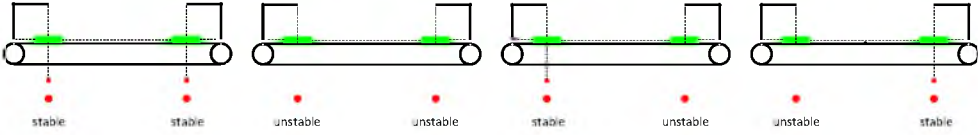

Figure 3. System configurations and the fixed points ($\mu_{1st} = \mu_{2st} = 0$, $\kappa_1 = \kappa_2 = 0$)
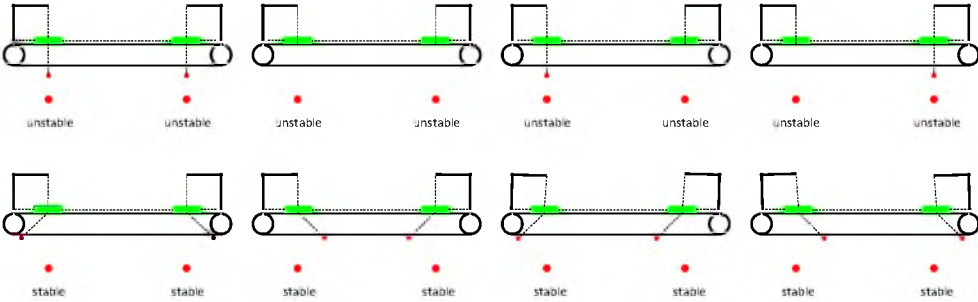

Figure 4. System configurations and the fixed points ($\mu_{1st} = \mu_{2st} = 0$, $\kappa_1 = \kappa_2 = 1\,\text{N}\cdot\text{m}^2$)

In the first case we have a situation of classical simple or inverted gravity pendulums (a stable equilibrium position of the simple pendulum and unstable equilibrium position of the inverted pendulum). In turn, in the cases of configurations of the system presented in Fig. 4, both simple or inverted pendulums in vertical positions are located in unstable positions. Between the mentioned unstable fixed points there are also fixed stable points.

In Figures 5-13 some chosen time histories of angles $\varphi_i(t)$ and trajectories of the point masses m_i are reported (values of the appropriate quantities are presented in SI units). Figures 5-8 illustrate different scenarios of transition of the system from initial conditions to stable fixed points. In the cases reported in Figs. 5 and 7, point masses m_i move from initial conditions to a near first unstable point (simple hanging pendulums placed in vertical positions), and finally reaching the first stable position. In the cases illustrated in Figs. 6 and 8, pendulums move from initial conditions, and oscillate near all stable and unstable fixed points, being finally attracted by one of the stable position.

The results reported in Figs. 9-10 show sensitivity of the considered system with respect to the parameters κ_1, κ_2 responsible for additional forces acting on the spring pendulums. Even a small change of these parameters push the considered pendulums to move from the initial conditions to the different fixed points.
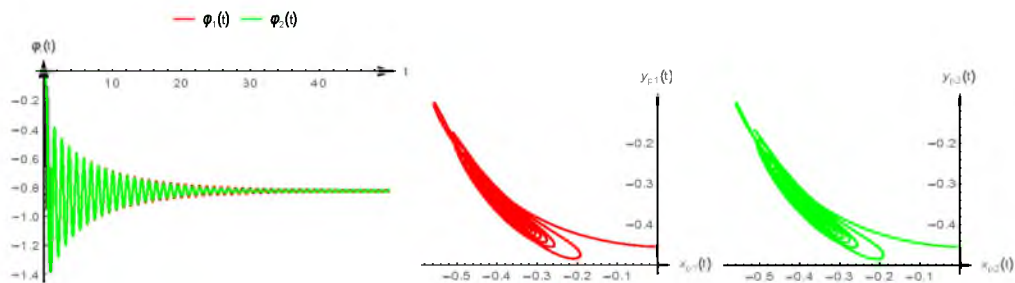
Figure 5. Time histories of angles $\varphi_i(t)$ and trajectories of the masses m_i (for initial parameters of the system)
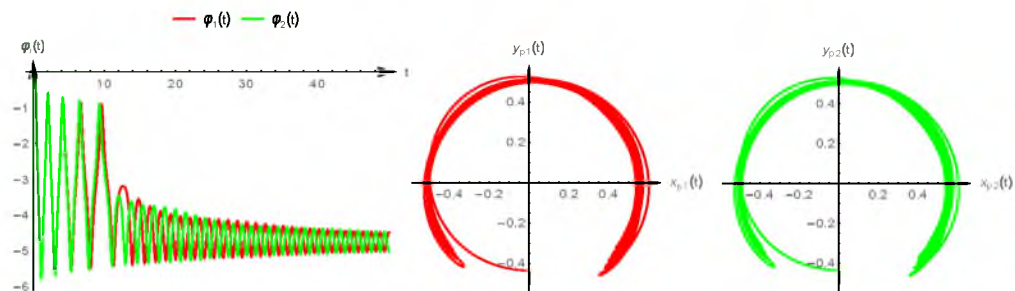

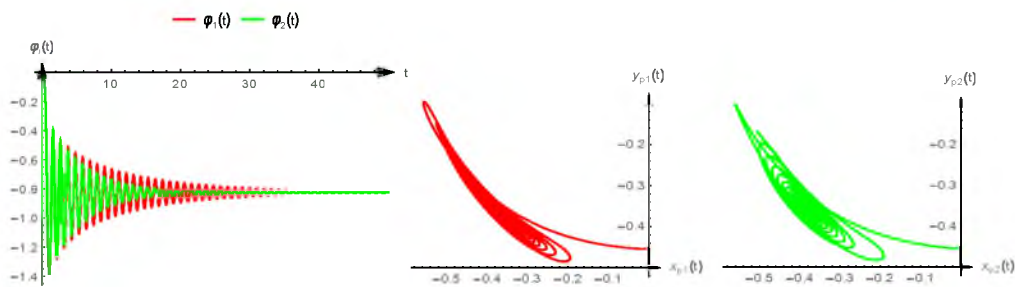**Figure 6.** Time histories of angles $\varphi_i(t)$ and trajectories of the masses m_i ($m_1 = m_2 = 0.1\,\mathrm{kg}$)

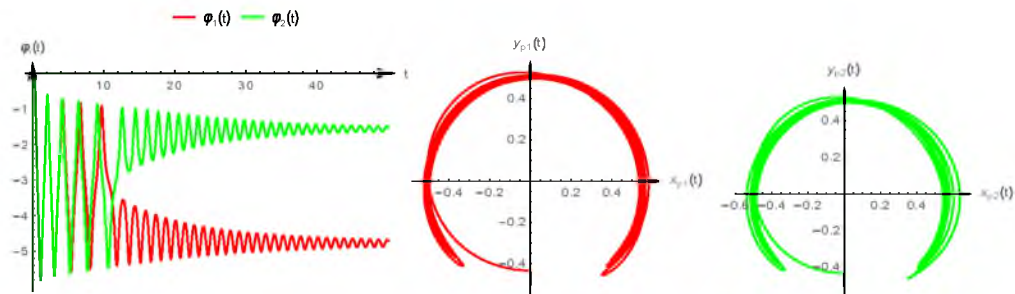**Figure 7.** Time histories of angles $\varphi_i(t)$ and trajectories of the masses m_i ($k = 0$, $c = 0$)

Figure 8. Time histories of angles $\varphi_i(t)$ and trajectories of the masses m_i
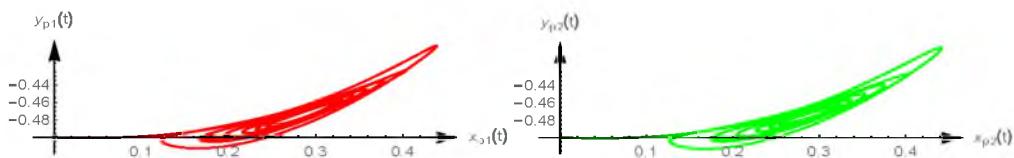($m_1 = m_2 = 0.1\,\mathrm{kg}$, $k = 0$, $c = 0$)

Figure 9. Trajectories of the masses m_i ($\kappa_1 = \kappa_2 = 0.35\,\mathrm{N\cdot m^2}$)
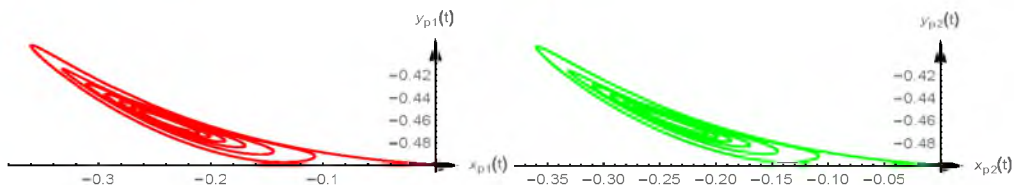

Figure 10. Trajectories of the masses m_i ($\kappa_1 = \kappa_2 = 0.36\,\mathrm{N\cdot m^2}$)

Figures 11-14 show time histories of angles $\varphi_i(t)$ for $m_1 = m_2 = 0.1\,\mathrm{kg}$, $\kappa_1 = \kappa_2 = 0.35\,\mathrm{N\cdot m^2}$ and different velocities v_{dr} of the belt. As can be seen, at the beginning spring pendulums oscillate in phase, after some time they oscillate in anti-phase, and this process vary in a periodic manner. This process is related to the energy exchange between the oscillators (pendulums). Movements of the individual pendulums can be regular or irregular, depending on the stick-slip vibrations occurring in the considered system.
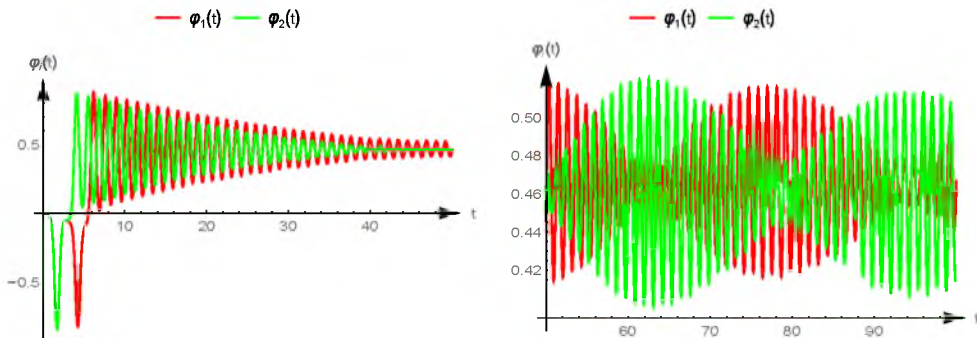

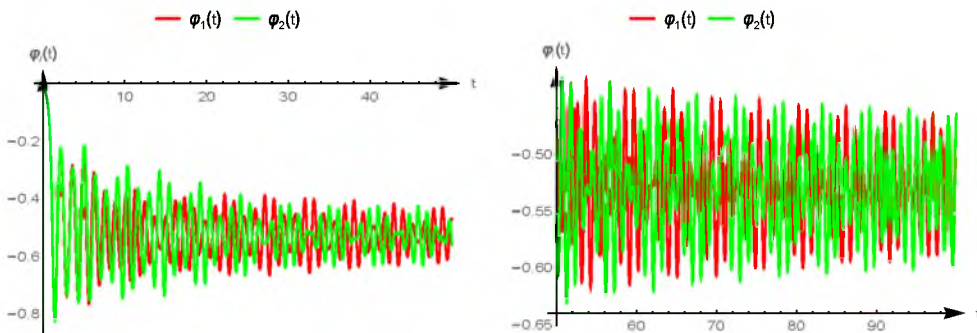**Figure 11.** Time histories of angles $\varphi_i(t)$ for $v_{dr} = 0.01\,\mathrm{m/s}$

Figure 12. Time histories of angles $\varphi_i(t)$ for $v_{dr} = 0.05\,\mathrm{m/s}$
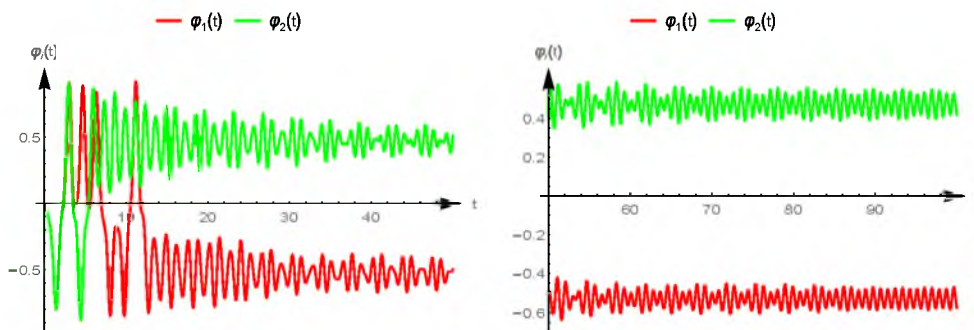
Figure 13. Time histories of angles $\varphi_i(t)$ for $v_{dr} = 0.1\,\text{m/s}$

Conclusions

In the paper dynamics of two coupled mechanical oscillators with spring pendulums and driven by a stick-slip induced vibrations are investigated. First, stable and unstable fixed points of the system are calculated analytically and numerically. Next, dynamical behaviours near fixed points are illustrated and discussed. Due to mathematical complexity (many degrees of freedom and discontinuities of equations of motion) the considered system is investigated numerically with a help of the Mathematical software. Numerical calculations are performed for certain set of parameters and initial conditions. As a result, a few nonlinear phenomena occurring for a narrow range of the parameters may be not detected. Analytical approach allows to obtain the solution as a function of some chosen parameters which gives the opportunity to discuss the results for full spectrum of the system parameters. However, the exact analytical or semi-analytical solution cannot be obtained due to nonlinearity, discontinuity and couplings in the equations of motion of the considered system. Our further research will be focused on analytical and/or numerical analysis of the considered system in the non-dimensional form, including resonance and synchronization effects, energy transition between oscillators, different scenarios of transition from regular to chaotic motion, bifurcation diagrams, Lyapunov exponents, power spectra densities, etc.).

Acknowledgments

References

[1]   Manevitch L.I., Musienko A.I. Limiting phase trajectories and energy exchange between anharmonic oscillator and external force *Nonlinear Dynamics*, 2009, Vol. 58, p. 633-642.
[2]   Starosvetsky Y., Gendelman O.V. Dynamics of a strongly nonlinear vibration absorber coupled to a harmonically excited two-degree-of-freedom system *Journal of Sound and Vibration*, 2008, Vol. 312, p. 234-256.
[3]   Awrejcewicz J., Starosta R. and Sypniewska-Kamińska G. Asymptotic analysis and limiting phase trajectories in the dynamics of spring pendulum. In: *Applied Non-Linear Dynamical Systems* Springer Proceedings in Mathematics & Statistics, 2014, Vol. 93, p. 161-173.